

Grand Solar Minima 1000-2100 A.D.

*Harald Yndestad,
NTNU Ålesund*

Update: 08.03.2020

*NTNU in Ålesund, Postboks 1517,
NO-6025 Ålesund, Norway*
<https://www.ntnu.edu/employees/harald.yndestad>

Summary

The wavelet spectrum analysis of solar activity from 1700 to 2020 reveals:

1. A stationary period spectrum of $n \cdot 11$ years for $n = 1, 2, 3, \dots$, in coincidence to the stationary 11.07-year Schwabe cycle, controlled by the planets Jupiter, Earth and Venus.
2. The 11.07-year specter has a 177.7-year coincidence resonance to the periods [88.56, 177.7] (yr). The periods are known as Gleissberg and Solar Barycenter resonance periods, controlled by the planets Saturn, Uranus and Neptune.
3. The identified dominant 178-year solar activity period has coincidences to known Grand solar minima from 1000 A.D.
4. The 89-year and the 178-year long periods have a 50-year positive phase-coincidence to maximum sola activity from 1933 to 1984 in a modern solar maximum activity period from 1925 to 2015.
5. The solar periods have minima coincidences from the years Fsa(2073) to Fsa(2103), computed minima at the years [2060, 2096] and a computed Grand deep minimum close to the year 2077 A.D.

1. Solar Activity

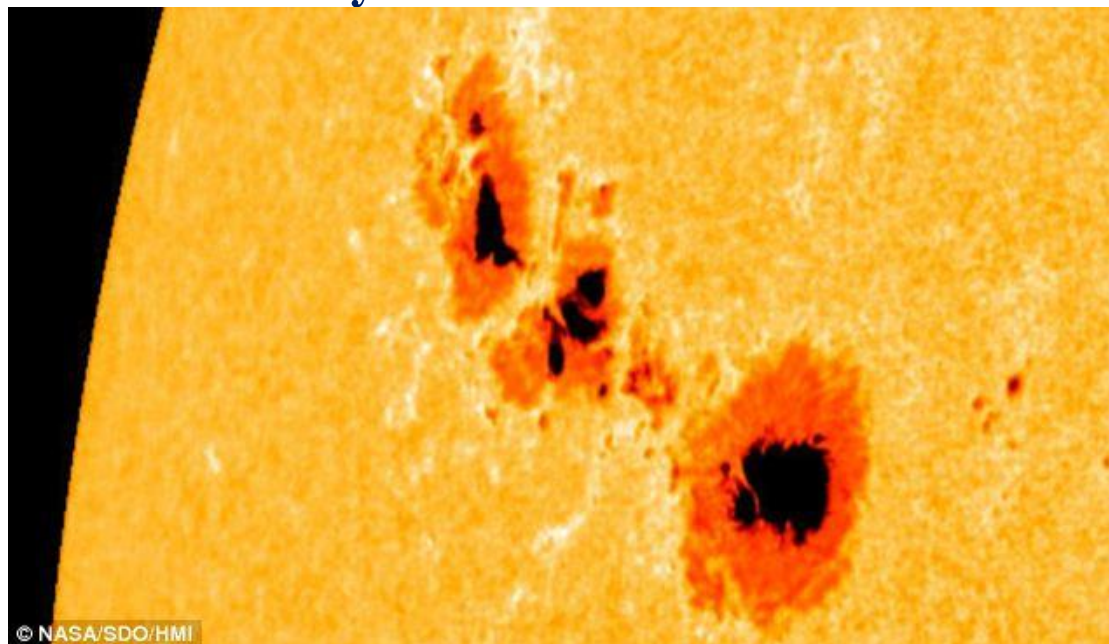


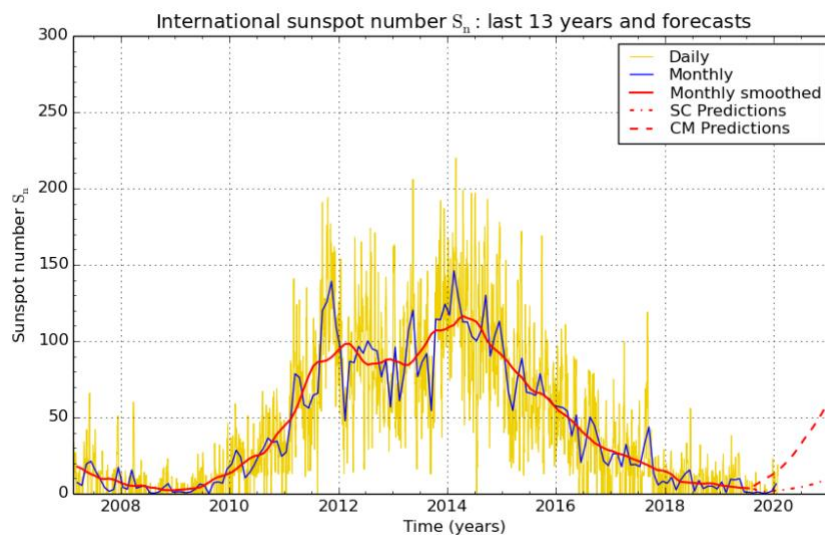
Figure 1. Sunspots on the Sun. <https://en.wikipedia.org/wiki/Sunspot>

The assumption that solar activity were immutable, as postulated by Aristotle (384-322 B.C.), was believed for millennia in numerous societies. Galileo Galilei resumed his observations of sunspots in April 1612. In his letters to Wesler, published in 1613, he identified sunspots correctly as markings on the sun, confirming that the sun rotated monthly, as the position of the spots moved. Although some transient changes of the Sun were observed with the naked eye, the introduction of the telescope in approximately 1600 demonstrated that the Sun possessed spots that varied in number and location. The sun has an activity and sunspots numbers became an indicator of solar activities.

From 1610, systematic observations were reported. A pattern of sunspot variations was established when Heinrich Schwabe began regular observations of sunspots in 1826. He reported a possible period of approximately ten years and presented the opinion that the planets Venus, Earth, Jupiter and Saturn modulate the solar variability. Rudolf Wolf started systematic observations of sunspot numbers in 1849. He also collected previous observations to construct daily sunspot numbers from 1750 and a yearly series from 1700. The cycle that started in 1755 became sunspot cycle 1.

The solar activity cycle (Hathaway, 2015) consists of dark sunspots and bright regions (faculae) in addition to active regions that exhibit sudden energy releases (flares). The average cycle length is 11.07 years. During a cycle, the number of spots increases to a maximum and then decreases. The average lifetime of a sunspot is slightly longer than the solar rotation period. They are bipolar, with the same magnetic polarity that leads with respect to the direction of the solar rotation. When the next cycle starts, spots appear with opposite polarity at high latitudes in both hemispheres, and as the cycle progresses, they appear closer to the equator (Yndestad and Solheim, 2019).

1.1 Solar activity cycles



SILSO graphics (<http://sidc.be/silso>) Royal Observatory of Belgium 2020 February 1

Figure 2: Solar activity cycle number 24 from 2008 to 2020. Source: WDC-SILSO, Royal Observatory of Belgium, Brussels. <http://www.sidc.be/silso/home>

Figure 2 shows the number of sunspots in solar activity cycle number 24 from 2008 to 2020. The time-variant number of sunspots may be represented by the simple model $Ssa(Ssn(), Asa(), Tsa(), Fsa())$, where $Ssn()$ represents the solar cycle number, $Asa(t)$ the time-variant amplitude, $Tsa()$ solar activity period time and $Fsa()$ the solar activity period phase state. The solar cycle 24 has sunspots minima at: $Ssa(Ssn(24), Asa(\min), Tsa(), (Fsa(2008), Fsa(2020)))$ in a period of $Tsa() = [Fsa(2020)] - Fsa(2008) = 11$ years and a maximum number $Ssa(Ssn(24), Asa(\max), Tsa(11), (Fsa(2014)))$ for $Asa(\max) = 125$ sunspot numbers.

If solar cycles have a stationary 11-year period, we may expect an upcoming next solar maximum and a minimum at the years: $Ssa((Ssn(22), Asa(\max), Tsa(11), (Fsa(2014) + 11 = 2025)))$ and $Ssa(Ssn(25), Asa(\min), Tsa(11), Fsa(2020+11 = 2031))$.

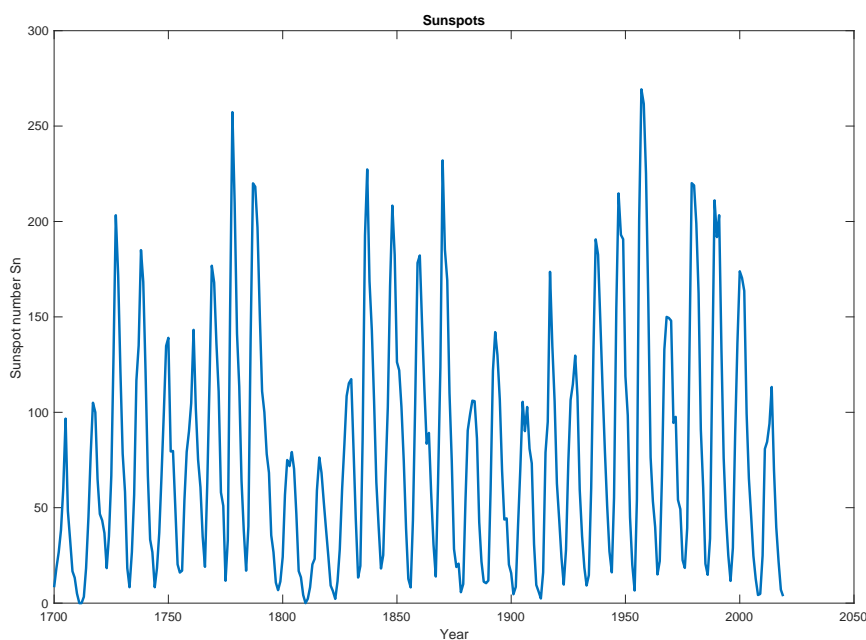


Figure 3: Solar activity from 1700-2020. Source: WDC-SILSO, Royal Observatory of Belgium, Brussels. <http://www.sidc.be/silso/home>

Figure 3 shows the number of sunspots in the solar activity from 1700 to 2020. In this time period the solar cycle numbers $S_{sn}()$ have a time-variant maximum number of sunspots $A_{ss(max)}$. The solar cycle number $S_{sn}()$ have smaller $A_{ss(max)}$ close to the years $[F_{sa}(1700), F_{sa}(1810), F_{sa}(1910), F_{sa}(2020)]$. These sunspots minima have a possible relation to reduced Total Solar Irradiation (TSI) from the Sun and colder climate on Earth.

1.2 Grand solar minima

As the sunspot data series became longer, it exhibited stationary 11-year periods and sunspot amplitude variability (Schwabe 1844). In the 1890s, G. Spörer and E. W. Maunder (1890) reported that solar activity greatly decreased during a cold period from 1645 to 1715 (Eddy 1974; 1973). Suess (1980) studied the radiocarbon dating of pine tree rings over the past 8,000 years and identified a stationary climate period of approximately 210 years. The 210-year climate oscillation coincided with the Maunder (1640–1720) and Dalton (1790–1820) (Usoskin et al. 2014) minimum solar variability periods, which stimulated speculation about the next possible cold climate period (Velasco and Mendoza 2008; Cliver et al. 1998). An adjustment-free reconstruction of the solar activity over the last three millennia confirms four Grand minima since the year 1000: [Oort (1010–1070), Wolf (1270–1340), Spörer (1390–1550), Maunder (1640–1720), Dalton(1790 - 1820)], (Usoskin et al., 2007). The Grand minima are associated with less solar activity and colder climate periods.

1.3 Total Solar Irradiation

Solar activity, represented by Sunspot numbers, may represent an indicator of Total Solar irradiation (TSI) from the Sun. Total solar irradiance represents a direct index for

the luminosity of the Sun measured at the average distance of the Earth. Since the beginning of satellite observations in 1979, the TSI has increased by approximately 0.1% from the solar minima to the solar maxima in the three satellite-observed sunspot cycles. A new study of solar activity shows a close relation between TSI from 1000 A.D, TSI from 1700 and Sunspots from 1610, show a coincidence between TSI variability, Sunspots variability and the planet periods of Saturn, Uranus and Neptune (Yndestad and Solheim, 2017).

2 Solar Variability

2.1 Stationary solar periods

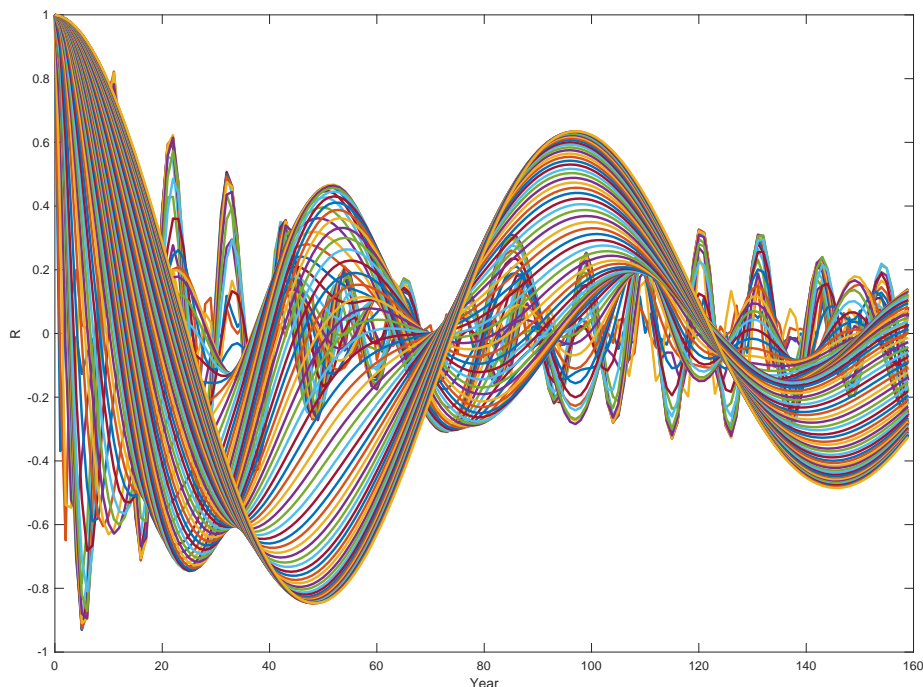


Figure 4. Solar activity wavelet autocorrelation spectrum $WAsa(R(s), m)$ for $s = 1 \dots 10$ and $t = 1700 \dots 2020$.

A wavelet transformation of sunspots numbers $Ssn()$ from 1700 to 2018 (Figure 5) computes a set of correlated periods $Wsa(s, t)$ to a set of moved scaled wavelet pulse function. Stationary periods in $Wsa(s, t)$ are identified by computing the autocorrelations $WAsa(R(s), m)$ [Eq. 4] as shown on Figure 4. The wavelet specter (Figure 4) has maxima period correlations of: $WAsa(Rsa, Tsa) = [(0.82, 11), (0.46, 52), (0.63, 96), (0.29, 180), (0.34, 200)]$ which show a correlation vector $Rsa() = [0.82, 0.46, 0.63, 0.29, 0.34]$ to the stationary close to the periods: $Tsa() = [11, 51, 96, 180, 200]$ (yr.).

2.2 Solar activity coincidence spectrum

The 11-year period has sub-harmonic periods of $Wsa(Rsa(s), Tsa) = [(0.60, 11), (0.50, 22), \dots]$, which confirm a stationary sola period close to $Tsa(11)$ years. The identified stationary periods in the solar activity spectrum have sub-harmonic coincidence periods of: $[5Tsa(11), Tsa(51)]$, $[8Tsa(11), Tsa(90)]$, $[10Tsa(11), 2Tsa(51), Tsa(110)]$, $[2Tsa(90), Tsa(180)]$, $[2Tsa(110), Tsa(220)]$ (yr).

2.3 Planet period coincidence

The planets Venus, Earth and Jupiter have a $[3, -5, 2]$ coincidence resonance of $Tvej = 22.14$ years, which confirm a $[2Tsa(11), Tvej(22.14)]$ coincidence between the sola periods and planet periods. The Jovian planets Jupiter, Saturn, Uranus and Neptune have a $[7, 3, 1, 1/2]$ coincidence resonance to identified 11-years period spectrum. Uranus and Neptune have position coincidences of $Tu(84.02) * Pn(164.79) / (Tn(164.79)) - Tu(84.02) = Tun(171.42)$ years. Tun(171.42) years and the Saturn period $5Ts(29.447)$ have a position coincidence period of $Tsun(177.77)$ years, which has a $[Tsun(177.77), Tvej(177.12)]$ coincidence.

The solar-planet periods have sub-harmonic coincidence periods of: $[[8Tsa(11), 4Tvej(22.14) = 88.56]$, $[(16Tsa(11), 8Tvej(22.14) = 177.12, Tsun(177.7)]$, $[20Tsa(11), 10Tvej(22.14) = 221.4]$. The identified 11-year spectrum has coincidences to the known periods Schwabe (11 years) cycle, Hale (22 year) cycle, Gleissberg (89 year) cycle, solar barycenter $Tsun(177.7)$ year cycle, Jose (179 year) cycle and the Suss/deVries (210 year) cycle.

2.4 Solar activity variations from 1700

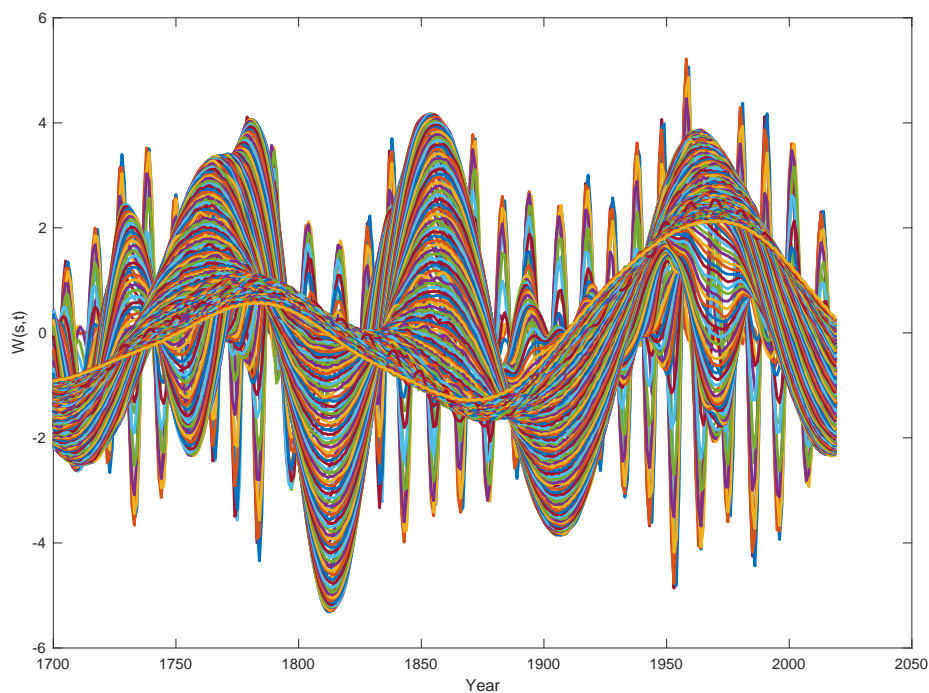


Figure 5. The Solar activity wavelet spectrum $W_{ss}(s, t)$ for $s = 1 \dots 130$ and $t = 1700 \dots 2020$.

The Sunspots data series (Figure 2) is transformed into a wavelet spectrum $W_{sa}(s, t)$ for $s = 1 \dots 130$ and $t = 1700 \dots 2020$ [Eq. 2] (Figure 5). The dominant period in the wavelet spectrum has amplitude and phase-shifts of: $W_{sa}(s(\max/\min), 0), F_{sa} = [(-0, 1743), (3.3, 1768), (+0, 1793), (-5.2, 1814), (-0, 1831), (4.2, 1854), (+0, 1878), (-3.7, 1908), (-0, 1932), (3.8, 1963), (+0, 2008)]$. The wavelet spectrum phase-shifts have mean distances of [25, (61, 21, 17, 23, 24, 30, 24, 31, 45] (yr). The longest period has phase-shifts of; $W_{sa}(s(\max/\min), 0), F_{sa} = [(-0, 1740), (0.6, 1782), (+0, 1825), (-1.2, 1869), (-0, 1911), (2.2, 1967), (+0, 2020)]$.

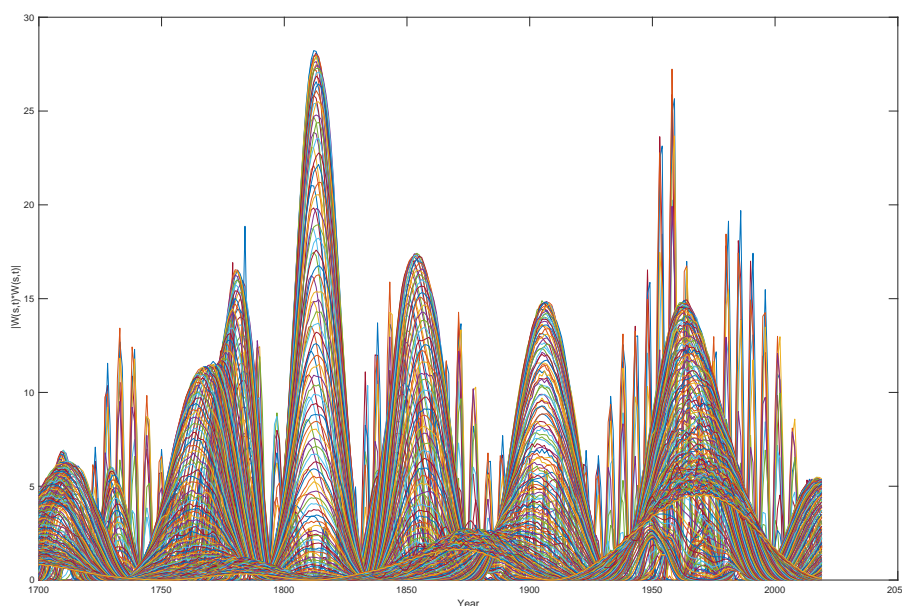


Figure 6. Solar activity wavelet power spectrum $W_{Ps_a}(s(t), t)$ for $t = 1700 \dots 2020$ and $s = 1 \dots 130$.

The wavelet power spectrum computes the most dominant period in the wavelet spectrum. The sunspots wavelet spectrum $W_{sa}(s, t)$ is transformed into a wavelet power spectrum $W_{Ps_a}(s, t)$ as shown on Figure 6. The computed wavelet power spectrum from 1700 to 2020 has a maximum and phase-shifts at the years: $W_{Ps_a}(s(\max), 0), T_{sa}(90), F_{sa} = [(-0, 1737), (11.2, 1770), (+0, 1796), (28.2, 1813), (-0, 1832), (17.4, 1854), (+0, 1877), (14.4, 1905), (-0, 1933), (14.8, 1962), (+0, 2015)]$. The wavelet power spectrum maximum has phase-shifts of [33, 26, 17, 19, 22, 23, 28, 29, 41] a mean time distance of 22.5 years and confirm mean total wavelet period of $T_{sa} = 4 * 22.5 = 90.0$ years, which confirm the 89-90 year period in solar activity. The longest period has wavelet phase-shifts of: $W_{Ps_a}(s(\min), 0), T_{sa}(176), F_{sa} = [(-0, 1752), (0.6, 1790), (+0, 1814), (-1.7, 1875), (-0, 1925), (1.9, 1967), (+0, 2015)]$ distances [38, 24, 61, 50, 42, 48] (yr) in a mean period $T_{sa}() = 175$ years, which confirm a 178-year Jose-period in solar activity.

Solar Activity model

The wavelet spectrum analysis identified the correlation vector: $R_{sa}() = [0.82, 0.63, 0.29]$ to the stationary close to the periods: $T_{sa}() = [11, 89, 178]$ (yr.). The periods have

maxima of: Ssa(Ssn(24), Asa(max), Tsa(11), (Fsa(2014)). Wsa(s(max), Tsa(90), Fsa) = [(14.8, 1962)] and Wpsa(Asa(max), Tsa(178), Fsa) = [(1.9, 1967)]. The identified correlations, periods and phaser-relations may represent the simplified model: Ssa(Asa(max), Tsa(), Fsa) = [(Asa(0.82), Tsa(11.07), Fsa(2014)), (Asa(0.64)), Tsa(89), Fsa(1962), (Asa(0.29), Tsa(178), Fsa(1967))]

2.5 Grand solar minima coincidences

Stationary periods, in coincidence to planet periods, are expected to have the same periods before 1700 and after 2020. We may then compute the coincidence between the identified [Tsa(90), Tss(175)] solar periods and known Grand solar minima from 1000 A.D., and we may compute expected upcoming Grand solar minima.

Dalton (1790 - 1820) coincidence: Wsa(Asa(0>), Tsa(90), Fsa) = [(+0, 1796), (-0, 1832)] and Wsa(Asa(0>), Tsa(175), Fsa) = [(+0, 1814), (min, 1813), (-0, 1925)] have minima coincidences from Fsa(1814) to Fsa(1832) in a period of 18 years. The period Tsa(175) has a 4 year Grand minimum coincidence from 1814 to 1820, which represents a short coincidence period.

Maunder (1640–1720) coincidence: Wsa(Asa(0>), Tsa(90), Fsa) = [(+0, 1616), (min, 1634), (-0, 1652)] and Wsa(Asa(0>), Tsa(175), Fsa) = [(+0, 1638), (min, 1694), (-0, 1749)] have minima coincidences from: 1638 to 1652 in a time-period of 14 years. The period Tss(175) has an 80 year Grand minimum coincidence from 1640 to 1720. The Tsa(175) period is close to a perfect Grand minimum coincidence.

Spörer (1390–1550), coincidence: Wsa(Asa(0>), Tsa(90), Fsa) = [(+0, 1436), (min, 1456), (-0, 1472)] and Wsa(Asa(0>), Tsa(175), Fsa) = [(+0, 1462), (min, 1506), (-0, 1550)] have minima coincidences from 1462 to 1472 in a time-period of 10 years. The period Tsa(175) has an 88 year Grand minimum coincidence from 1462 to 1550. The Tsa(175) period has a perfect Grand minimum coincidence.

Wolf (1270–1340) coincidence: Wsa(Asa(0>), Tsa(90), Fsa) = [(+0, 1256), (min, 1274), (-0, 1292)] and Wsa(Asa(0>), Tsa(176), Fsa) = [(+0, 1286), (min, 1380), (-0, 1474)] have minima coincidences from Fsa(1286) to Fsa(1292) in a period of 6 years. The long period Tsa(175) has a 54 year Grand minimum coincidence from 1286 to 1340.

Oort (1010–1070) coincidence: Wsa(Asa(0>), Tsa(90), Fss) = [(+0, 1076), (min, 1094), (-0, 1112)] and Wsa(Asa(0>), Tsa(176), Fsa) = [(+0, 1110), (min, 1203), (-0, 1298)], have minima coincidences from 1110 to 1112 in a time-period of 2 years. The long period Tsa(175) has a 60 year Grand minimum coincidence from 1010 to 1070, which is close to the Wolf type Grand minimum.

The computed phase-shifts reveals a close relation between the identified period Tsa(175) and Grand minima from 1000 A.D. A more accurate relation is most likely related to the solar Barycenter period Tsun(177.77) and the period 4Tvej(22.14) = 88.56).

Modern solar maximum coincidence: $Wsa(Asa(>0), Tsa(90), Fsa) = [(-0, 1933), (max, 1968), (+0, 1984)]$ and $Wsa(Asa(>0), Tsa(190), Fsa) = [(-0, 1925), (max, 1962), (+0, 2015)]$ have a 70-year positive coincidence period from 1933 to 1984, which explain a 50-year period of maximum solar activity. The solar activity period $Tsa(175)$ positive state from 1925 to 2015 reveals the end of modern solar maximum at the year 2015 and reveals the beginning of an upcoming next Grand minimum period.

Upcoming next Grand solar minimum: $Wsa(Asa(>0), Tsa(90), Fsa) = [(+0, 2073), (min, 2095), (-0, 2117)]$ and $Wsa(Asa(>0), Tsa(176), Fsa) = [(+0, 2015), (min, 2060), (-0, 2103), (max, 2150)]$ have minima coincidences from the years $Fsa(2073)$ to $Fsa(2103)$ in a period of 30 years. The periods have computed minima at the years [2060, 2096] and a computed Grand deep minimum close to the year 2077 A.D.

3 Discussion

A wavelet spectrum analysis of sunspot group numbers from 1611 identified solar-Uranus period coincidences of $[5Tsa(11), (2Tur(84.02)/3 = 56.0), (10Tsa(11), 4Tur(84.02)/3 = 112.0), (20Tsa(11), 5Tn(84.02)/2 = 210.0)]$. The Jovian planets Jupiter, Saturn, Uranus and Neptune have a $[7, 3, 1, 1/2]$ coincidence resonance, which confirms a coincidence resonance between the 11-year spectrum and the Jovian planets. (Yndestad and Solheim, 2017). The new information from this investigation is the solar activity coincidence periods of: $[[8Tsa(11), 4Tvej(22.14) = 88.56], [16Tsa(11), 8Tvej(22.14) = 177.12, Tsun(177.7)], [20Tsa(11), 10Tvej(22.14) = 221.4]]$, known as the the Schwabe (11 years) cycle, Hale (22 year) cycle, Gleissberg (89 year) cycle, solar Barycenter (177.7 year) cycle, Jose (179 year) cycle and the Suss/deVries (210 year) cycle.

The implication of the coincidence between solar activity variability and the planet periods is deterministic long periods in the solar activity. We may then compute expected upcoming maxima and Grand minima solar activity. A possible explanation is the coincidence between planet period-phase relations and solar Barycenter periods, which influences the solar dynamo and the solar activity on the Sun surface. The identified 178-year Barycenter period and solar period have a coincidence to known Grand minima from 1000 A.D. confirm a stationary Grand minima period close to the 178-year Barycenter period of the Jovial planets.

The solar activity variability has a coincidence to Total Solar Irradiation and climate periods. An analysis of the ACRIM-HS and ACRIM-LS TSI data series computer TSI solar minimum periods from $[(2035-2065), (2045-2070)]$ and computed deep minima at the years [2049, 2060] (Yndestad and Solheim 2017). This investigation has identified a coincidence between the modern warm period from 1933 to 2015, reduced solar activity period from 2015 to 2103 and a deep solar Grand activity minimum close to the period 2060-2100 A.D.

4 Methods

To reduce false periods, all data series are scaled prior to the wavelet analysis by the following:

$$x(t) = y(t) - E[y(t)]/\text{var}[y(t)] \quad (1)$$

where $y(t)$ is the data series, $E[y(t)]$ is the mean value, $\text{var}[y(t)]$ is the variance and $x(t)$ is the scaled data series. The scaled data series are transformed into a wavelet spectrum by the following:

$$W_{a,b}(t) = \frac{1}{\sqrt{a}} \int_R x(t) \Psi\left(\frac{t-b}{a}\right) dt \quad (2)$$

where $x(t)$ is the analyzed time series; $\Psi()$ is a `coif3` wavelet impulse function [63], [64], which is chosen for its symmetrical performance and its ability to identify symmetrical periods in data series; $W_{a,b}(t)$ represents the computed wavelet spectrum; parameter a represents a time-scaling parameter; and parameter b represents a translation in time for the wavelet transformation. When translating $b = 0$ and $s = 1/a$, the wavelet spectrum $W(s, t)$ represents a set of moving correlations between $x(t)$ and the impulse function $\Psi()$ over the entire time series $x(t)$. The relationship between wavelet s and sinus period T is approximately $T \approx 1.2 s$ when using the `coif3` wavelet function. In this investigation, the transformed wavelet spectrum $W(s, t)$ has a set of wavelet functions in the spectrum range $s = 0, 1, 2 \dots 0.6N$, where N is the number of samples in the data series. $W(s(\text{min}), -0, \text{max}, +0), F)$ represents a wavelet s that has a dominant phase state $W(s(\text{max}), F) = [\text{min}, -0, \text{max}, \text{or } +0]$, at a year $t = F$. The wavelet power spectrum is computed by the following transform:

$$\text{WP}(s, t) = W(s, t) * W(s, t) \quad (3)$$

The wavelet power spectrum identifies the most dominant wavelets in the wavelet spectrum $W(s, t)$. $\text{WP}(s(\text{max}) F) = [s(\text{min}), -0, \text{max}, +0], F)$ represents a wavelet power spectrum where the maximum amplitude has phase-shifts $[\text{min}, -0, \text{max}, +0]$ at the time vector F (yr.). A wavelet spectrum $W(s, t)$ is transformed into a set of autocorrelations by the following transform:

$$\text{WA}(R(s), m) = E[W(s, t)W(s, t + m)] \quad (4)$$

where $\text{WA}(R(\text{max}), T) = (R, T)$ represents a wavelet s that has a correlation R to a stationary period T . A stationary period T in $\text{WA}(R(s), m)$ has a set of subharmonic periods at $m = [T, 2T, 3T \dots]$ (yr.). A set of autocorrelations may have coincidence periods of $\text{WA}(R(\text{max}), m) = [(R1, k*T1), (R2, p*T2)]$ for $k*T1 = p*T2$. Stationary are identified by computing the period- and phase difference:

$$E(Ae, Te, Fe) = [S(Aa, Ta, Fa) - S(Ab, Tb, Fb)] \quad (5)$$

where $S(Ae, Te, Fe)$ represents a period spectrum from an unknown source.

References

- Eddy, J.A., 1976. The maunder minimum. *Sci.* 192, 1189–1202.
- Eddy, J.A., 1983. The maunder minimum a reappraisal. *Sol. Phys.* 89, 195–207. doi: 10007/BF00211962.
- Schwabe, H., 1844. Sonnen-beobactungen im jahre 1843. *Astron. Nachr.* 21 (495), 233–236.
- Hathaway, D.H., 2015, The Solar Cycle, *Living Rev. Sol. Phys.*, 12,(4).
- Maunder, E.W., 1890. Professor spoerer's researches on sun-spots. *MNRAS* 50, 251–252.
- McCracken, K.G., Beer, J., Steinhilber, F., 2014. Evidence for planetary forcing of the cosmic ray intensity and solar activity throughout the past 9400 years. *Sol. Phys.* 289, 3207–3229. doi:10.1007/s11207-014-0510-1.
- Velasco, V.M., Mendoza, B., 2008. Assessing the relationship between solar activity and some large scale climatic phenomena. *Adv. Space Res.* 42, 866–878. doi:10.1016/j.asr.2007.05.050.
- Usoskin, I.G., et al., 2014. Evidence for distinct modes of solar activity. *As& A* 562. L10. doi: 10.1051/0004-6361/201423391.
- Yndestad, H., & Solheim, J. (2017). The influence of solar system oscillation on the variability of the total solar irradiance. *New Astronomy*, 51, 135–152. <http://doi.org/10.1016/j.newast.2016.08.020>